Published in final edited form as:
Dev Dyn. 2010 March ; 239(3): 763–772. doi:10.1002/dvdy.22205.

Analysis of conserved residues in the β*pat-3* cytoplasmic tail reveals important functions of integrin in multiple tissues

Xiaojian Xu[1], **Jeong H. Ahn**[1], **Phebe Tam**[1], **Eun Jeong Yu**[1], **Sushil Batra**[1], **Erin J. Cram**[2,*], and **Myeongwoo Lee**[1,*]

[1] Department of Biology, Baylor University, One Bear Place 97388, Waco, TX 76798

[2] Department of Biology, Northeastern University, 360 Huntington Ave, Boston, MA 02115, U.S.A

Abstract

Integrin cytoplasmic tails contain motifs that link extracelluar information to cell behavior such as cell migration and contraction. To investigate the cell functions mediated by the conserved motifs, we created mutations in the *Caenorhabditis elegans* β*pat-3* cytoplasmic tail. The β1D (^{799}FK^{800}), NPXY, tryptophan (^{784}W), and threonine (^{797}TT^{798}) motifs were disrupted to identify their functions *in vivo*. Animals expressing integrins with disrupted NPXY motifs were viable, but displayed distal tip cell migration and ovulation defects. The conserved threonines were required for gonad migration and contraction as well as tail morphogenesis, whereas disruption of the β1D and tryptophan motifs produced only mild defects. To abolish multiple conserved motifs, a β1C-like variant, which results in a frameshift, was constructed. β*pat-3*(β1C) transgenic animals showed cold-sensitive larval arrests and defective muscle structure and gonad migration and contraction. Our study suggests that the conserved NPXY and TT motifs play important roles in tissue-specific function of integrin.

Keywords

Integrin; conserved tyrosine; DTC migration; cytoplasmic tail; gonad; ovulation; frameshift mutations; cold-sensitive; beta 1C integrin; NPXY motif

Introduction

Integrins are heterodimeric transmembrane receptors for extracellular matrix (ECM). In mammals, there are more than 20 different integrin molecules, which are composed of combinations of α and β genes (Hynes, 1992; Hynes, 2002). Integrins bind ECM molecules such as collagens, fibronectin, and laminin and assemble a cytoplasmic protein complex known as a focal adhesion, which includes both structural and signaling components. This integrin-mediated linkage is crucial for the proper control of cell behaviors such as cell migration, adhesion, differentiation, and death (Giancotti, 1997; Giancotti and Ruoslahti, 1999).

Caenorhabditis elegans is an excellent model system with which to study the developmental function of integrins because it only possesses two integrin heterodimers composed of one α (INA-1 or PAT-2) and one β (PAT-3) integrin subunit (Kramer, 2005). Null alleles of α*pat-2* and β*pat-3* result in the paralyzed and arrested at two-fold embryonic lethality phenotype (Pat) (Williams and Waterston, 1994), and loss of α*ina-1* results in larval lethal (Baum and

[*]All correspondence should be addressed to: Erin J. Cram, Ph.D., Tel) 617-373-7533, e.cram@neu.edu or Myeongwoo Lee, Ph.D., TEL) 254-710-2135, myeongwoo_lee@baylor.edu.

Garriga, 1997). βPAT-3 integrin likely forms a heterodimer with αPAT-2 or αINA-1 and controls many cellular events during *C. elegans* development. βPAT-3 integrin is expressed in the body wall and sex muscles, embryonic pharynx, spermatheca, uterus, somatic gonad, and neurons (Gettner et al., 1995). βPAT-3/αPAT-2 heterodimers are expressed in many tissues including muscles and somatic gonad whereas βPAT-3/αINA-1 pairs are localized mainly to migratory cells such as distal tip cells (DTC) and neurons (Lee et al., 2001; Cram et al., 2003; Meighan and Schwarzbauer, 2007).

In body wall muscle cells, integrins are localized in dense bodies (Z band analog) and M-lines, anchoring sarcomeres to the adjacent basement membrane (BM), a specialized ECM encompassing muscles and gonad, and play essential roles in stabilizing the muscle attachment structures (Moerman and Williams, 2006). Genetic screens have isolated several *βpat-3* mutations including null and reduction-of-function alleles (Williams and Waterston, 1994; Gettner et al., 1995). However, all available *βpat-3* mutations are within in the extracellular domain, limiting the analysis of its intracellular function (Gettner, 1994).

Functional analysis of *βpat-3* integrin using a dominant negative HA-βtail revealed that inhibition of *βpat-3* cytoplasmic tail function caused gonad migration and ovulation defects, suggesting an important role for *βpat-3* integrin in cell migration and contraction (Lee et al., 2001; Lee et al., 2005). In addition, RNA mediated interference (RNAi) of *βpat-3* results in disorganized F-actin in muscle, defective DTC migration (Cram et al., 2003; Cram et al., 2006) and contractile defects of the myoepithelial cells of the somatic gonad, demonstrating the essential role of cell-ECM interaction in organization and function of these tissues (Lee et al., 2005; Sherwood et al., 2005; Xu et al., 2006).

βPAT-3 integrin is well conserved relative to human β1 integrin (61% protein sequence similarity) and shares many conserved motifs (Figure 1). Essential residues such as an aspartic acid (^{768}D in βPAT-3) that forms a salt bridge to the α partner, a conserved domain (^{761}K to ^{775}F) that mediates focal adhesion kinase (FAK) or paxillin binding, and the talin binding (^{784}W to ^{800}K) sites are all conserved in βPAT-3 (Figure 1). The two NPXY (asp-pro-X-tyr) motifs are also conserved in βPAT-3 tail (Lee et al., 2001). Tyrosine phosphorylation of NPXY leads to integrin activation and promotes interactions with downstream signaling molecules including talin, ICAP-1, and kindlins (Calderwood et al., 2002;Zawistowski et al., 2002;Calderwood, 2004;Oxley et al., 2008;Harburger et al., 2009). Functional studies of NPXY motifs in mouse β3 integrin showed that platelets displayed defective chemotaxis when one or both Y was changed to F (Law et al., 1999). The Y to alanine (A) mutation in mouse β1 or β3 integrin abolishes integrin functions and results in embryonic lethality (Chen et al., 2006). Disrupting the two NPXY motifs impaired the proliferation and survival of mouse embryonic fibroblasts (MEF) (Hirsch et al., 2002).

In a previous study, we determined the role of the conserved NPXY motifs in the cytoplasmic domain of βPAT-3. Two rescued lines, β*pat-3*(Y804F) and β*pat-3*(YYFF), rescued the embryonic lethality of *βpat-3*(*st564)* and generated viable and fertile progeny (Lee et al., 2001). These transgenic animals exhibited mild defects in distal tip cell migration. Most commonly, the DTC turned away from the dorsal surface and returned to the ventral side, perhaps because of defective adhesion to the dorsal body wall basement membrane (Lee et al., 2001). Immunofluorescence staining of rescued animals with MH25, a monoclonal antibody against βPAT-3, demonstrated normal localization and distribution of dense bodies (Francis and Waterston, 1991; Lee et al., 2001). Muscle filamentous actin staining in the rescued NPXY lines was also indistinguishable from β*pat-3* (+) animals (Lee et al., 2001). These data suggested that the NPXY motif may play an important role in cell migration but is not required for muscle cell organization.

In this study we have extended our analysis of conserved motifs, β*pat-3*(TTAA), β*pat-3*(W784A), β*pat-3*(FKVV), and a splice mutant β*pat-3*(β1C), in the cytoplasmic tail of βPAT-3 and compared them to our previous results targeting the NPXY motifs. All of our transgenic rescue constructs can rescue the embryonic lethality of the *βpat-3(st564)* null allele (Williams and Waterston, 1994), but displayed multiple larval and adult phenotypes caused by defective integrin function. Disruption of specific integrin motifs results in defects in DTC migration, ovulation, and muscle cell function. Importantly, we identify a novel role for integrin in hermaphrodite tail morphogenesis.

Results

Targeting conserved motifs in the β integrin cytoplasmic tail

To study the role of the conserved amino acid residues and motifsessential for integrin function in embryonic and post-embryonic development, *C. elegans* strains with point mutations in conserved motifs in the cytoplasmic domain of β*pat-3* were established (Figure 1A). All constructs were created by PCR mutagenesis, purified, and injected into balanced *βpat-3(st564)* heterozygous animals to produce rescued transgenic lines in which animals are dependent on the transgene for survival.

There are two NPXY motifs that include the tyrosines Y^{792} and Y^{804} in βPAT-3 tail (Chen et al., 1990; Lee et al., 2001). Tyrosine phosphorylation of the NPXY motif is thought to activate integrin and promote interactions with downstream signaling molecules (Calderwood et al., 2002). This motif has been shown to be important for integrin function in fly (Zusman et al., 1990; Zusman et al., 1993; Jannuzi et al., 2002; Jannuzi et al., 2004), worm (Lee et al., 2001), mouse (Czuchra et al., 2006), and mammalian tissue culture (Sakai et al., 1998; Kaapa et al., 1999). We have previously demonstrated that disruption of the NPXY motifs, either singly (Y804F) or in combination (YYFF) leads to defects in the rescued transgenic lines including DTC migration defects (Lee et al., 2001). In order to further characterize the importance of phosophorylation in the NPXY motif, we generated a point mutation in Y^{792} for this study, and compare the effects of disruption of these NPXY motifs to a new set of point mutations targeting conserved residues in the βPAT-3 cytoplasmic domain.

The three new motifs targeted for analysis are a ^{799}FK^{800} motif, a tryptophan motif ^{784}WDT^{786}, and a threonine motif ^{797}TT^{798}. In order to determine the *in vivo* importance of these sequences, we have generated rescued transgenic lines expressing *βpat-3* with point mutations disrupting these residues. An identical sequence to βPAT-3 (^{799}FKNPXY^{804})is found in the muscle integrin β1D (Figure 1B), a splice isoform of mammalian β1 integrin (Belkin et al., 1997; Belkin and Retta, 1998), whereas the sequence is ^{790}VVNPXY^{795} in human β1A, a splice isoform abundant in focal adhesions (Argraves et al., 1987), of β1 integrin. We generated rescued transgenic lines expressing ^{799}VVNPXY^{804}, and designated this line β*pat-3* (FKVV). The tryptophan (W) residue at the position 775 of human β1 integrin has been identified as necessary for integrin-mediated protein kinase B/Akt survival signaling (Pankov et al., 2003). Similar to human β1, βPAT-3 possesses the ^{784}WDT^{786} motif upstream of the first NPXY. The ^{784}W residue was mutated to alanine (A) and used to establish rescued transgenic nematodes, designated β*pat-3* (W784A). In mouse GD25 cells, mutations in the ^{788}TT^{789} motif of β1 integrin caused defective cell attachment to fibronectin and induced a shift to inactive conformation in the extracellular domain (Wennerberg et al., 1998), suggesting that these residues play important roles in the inside-out integrin signaling by relaying conformational change of cytoplasmic tail to the extracellular domain causing high affinity ligand binding (Tanentzapf and Brown, 2006). The threonines (^{797}TT^{798}) of β*pat-3* were mutated to alanine to produce ^{797}AA^{798} mutant designatedβ*pat-3*(TTAA) (Figure 1).

In addition, we have analyzed a nematode strain expressing βPAT-3 with significantly disrupted cytoplasmic tail sequences. In mammals, β1C integrin is an alternatively spliced form of the β1 subfamily that contains a unique 42-amino acid sequence in the cytoplasmic tail (Figure 1A). The β1C variant inhibits the growth of prostate cancer epithelial cells (Fornaro et al., 1998), endothelial cells (Meredith et al., 1995), and fibroblasts (Fornaro et al., 1995; Fornaro et al., 2000), is usually expressed in non-proliferative epithelium, and downregulated in prostate adenocarcinoma and proliferating breast carcinoma (Manzotti et al., 2000). We designed a mutant β*pat-3* gene, pPAT3-β1C, carrying a mutation (a**g** to a**a**) in the splice acceptor sequence of pPAT3(+) intron 7, which creates a frameshift in the ORF of β*pat-3* gene. Although the splicing defect in β*pat-3*(β1C) is not predicted to result in a homologous sequence to that found in the human β1C variant, in both cases all conserved motifs are disrupted. Inferred protein sequences of the cytoplasmic tails of all rescue constructs are indicated in Figure 1A. Rescued lines, able to rescue the embryonic lethality of *st564*, were established for each construct.

Severe disruption of the β*pat-3* cytoplasmic tail leads to defective muscle structure

Because integrin is localized to body wall muscles and involved in assembly and stabilization of contractile structures (Kramer, 1997; Kramer, 2005), we determined the localization of βPAT-3 and arrangement of dense bodies in the rescued lines using immunofluorescence. In the β*pat-3* (+) animals, βPAT-3 is localized to dotted and continuous lines along the length of muscle cells, typical of dense bodies (Figure 2). Immunostaining was performed on all rescued lines, and all were indistinguishable from wild type. Representative staining of β*pat-3*(Y792F) and β*pat-3*(β1C) is shown in Figure 2. The actin cytoskeleton was also visualized in mutant lines by staining with rhodamine-conjugated phalloidin. All of the rescued lines showed a normal staining pattern of dense bodies and actin filaments except for the frameshift line β*pat-3* (β1C) (Figure 3). These data suggest that the function of ^{799}FK^{800}, ^{784}WDT^{786}, and ^{797}TT^{798} motifs are dispensable for dense body organization and for organization of the actin cytoskeleton in muscle cells. This result is somewhat unexpected because FK motif is specifically found in a muscle specific splice form of mammalian integrin β1D (Belkin et al., 1997; Belkin and Retta, 1998), and the TT motif plays an important role in integrin activation and matrix binding in mouse cell culture (Wennerberg et al., 1998).

Consistent with genetic studies of *βpat-3* (Lee et al., 2001; Lee et al., 2005), significant disruption of βPAT-3 structure does result in muscle defects. β*pat-3* (β1C) transgenic animals were stained with MH25 and phalloidin to localize β*pat-3* and visualize the actin cytoskeleton. The majority of muscle cells appeared to have normal β*pat-3* localization and a regular pattern of filamentous actin staining. However, in some muscle cells, the actin cytoskeleton were clumped irregularly (Figure 2), suggesting that expression of the transgene can cause cytoskeletal defects. In *C. elegans*, disruption of splice junctions often results in temperature sensitive alleles, because splicing occurs inefficiently at 15° C (Aroian et al., 1990; Aroian and Sternberg, 1991; Aroian et al., 1993). Therefore, we investigated the cold sensitivity of the β*pat-3*(β1C) lines. At 15°C, a significant proportion of the animals were paralyzed and arrested after hatching, whereas at 23°C, the animals hatched and moved normally (Table 1). Arrested L1 larvae were stained with phalloidin and appeared to have muscle striations, although the actin seemed disorganized compared to normal L1 larvae (Figure 4).

To determine if β*pat-3*(β1C) can act in a dominant negative fashion at 15°C, the transgene was crossed into the wildtype (N2) background. The resulting β*pat-3*(β1C)/+ animals showed significant larval arrest at 15°C (58% larval arrest, N=76). A lower percentage of β*pat-3*(+)/+ heterozygotes displayed larval defects at the cold temperature (22% larval arrest, N=41). We then investigated the molecular basis of the cold sensitive phenotype of

βpat-3(β1C). RT-PCR was conducted on total RNA extracted from wild type (N2) and β*pat-3*(β1C) animals. Two different species of cDNA were detected and sequenced (Figure 4). RT-PCR conducted on rescued β*pat-3*(+) animals revealed correctly spliced transcripts indistinguishable from N2 (data not shown). The mutant, incorrectly spliced cDNA contained 53 bp of sequence derived from intron 7, whereas the smaller one contained no intron sequences. Therefore, β*pat-3* (β1C) animals express at least two *βpat-3* splice variants. Quantitative PCR (qPCR) analysis of *pat-3* transcripts indicates that in β*pat-3*(β1C) animals raised at 15° C, *pat-3* levels are elevated six-fold as compared to *pat-3* levels in animals raised at 23° C. This increase may be due to an increase in the unspliced form, because neither N2 nor rescued *pat-3* (+) animals show any increase in *pat-3* transcript at the non-permissive temperature. Taken together, these results suggest that β*pat-3*(β1C) tail produces two different species of βPAT-3 protein, one of which, presumably the mutant one, causes cold sensitivity and disrupts integrin functions.

Conserved residues in β*pat-3* cytoplasmic tail are important for DTC migration

During *C. elegans* development, the two hermaphrodite gonad arms elongate to form a mirror-image U-shaped structure (Hubbard and Greenstein, 2000). This elongation and migration is navigated by a pair of distal tip cells (DTC), specialized leader cells at the distal tip of each gonad arm (Montell, 1999; Nishiwaki, 1999; Hubbard and Greenstein, 2000). The NPXY motifs have previously been shown to be required for correct DTC pathfinding, and potentially adhesion, during DTC migration along the dorsal basement membrane (Lee et al., 2001) (Figure 5). As expected, β*pat-3*(Y804F) and β*pat-3*(YYFF) exhibited mild defects in DTC migration, and were significantly more affected than β*pat-3* (+). In many of these animals, distal gonad arms wandered out of the regular trajectory and collapsed toward the ventral side. Defects also included DTC migration from the dorsal to the ventral side near the proximal gonad, suggesting either abnormal pathfinding or loss of contacts with the dorsal body wall (Figure 5C). Disruption of the first NPXY motif in the β*pat-3*(Y792F) animals produced a milder effect on DTC migration than seen in the β*pat-3*(Y792F) and β*pat-3(*YYFF) lines. Although defects were consistently observed, the penetrance of defects was not significantly different from β*pat-3*(+) lines. The β*pat-3*(β1C) animals grown at 15°C showed DTC migration defects that were much more severe than β*pat-3*(β1C) animals grown at room temperature (Figure 5B, Table 1). DTC migration in β*pat-3*(β1C) at 15°C was also significantly more disrupted than any of the NPXF lines (Figure 5B, Table 1).

Disruption of the TT motif in the β*pat-3* tail also resulted in DTC migration defects. The β*pat-3*(TTAA) rescued lines had a much higher penetrance of DTC migration defects than β*pat-3(*+) (Table 1, Figure 4). In contrast, the β*pat-3*(FKVV) and β*pat-3*(W784A) transgenic lines exhibited mild DTC migration defects not significantly different from those observed in β*pat-3* (+) rescued animals. These results indicate that the ^{797}TT^{798} residues are important for proper pathfinding of the DTC, possibly more so than phosphorylation of the NPXY motif, or presence of the FK or WDT motifs. The DTC migration defects in β*pat-3*(TTAA) animals include incorrect pathfinding along the dorsal surface and supernumerary turns (Figure 5, Table 1). In cell culture, β1A integrin lacking the TT motif remained inactive and did not contribute to matrix binding or matrix remodeling (Wennerberg et al., 1998). Our results suggest that similarly, the TT motif may be required for the integrin-mediated extracellular matrix interaction important for correct DTC migration. Taken together, our analysis suggests that, while not essential for viability, multiple motifs within the βPAT-3 tail are required for optimal control of DTC migration.

Disruption of conserved residues in PAT-3 cytoplasmic tail leads to defects in ovulation and reduced fertility

Our previous studies have demonstrated that RNAi of *βpat-3* results in defective contraction of the gonad sheath cells and spermatheca. In these animals, oocytes accumulate in the proximal gonad because of failed ovulation (Lee et al., 2001; Xu et al., 2005; Xu et al., 2006). In this study, theβ*pat-3*(Y792F), β*pat-3*(Y804F), β*pat-3*(TTAA) and β*pat-3*(β1C) transgenic strains also exhibited defective ovulation (Figure 6). In these animals, oocytes were observed in a non-linear arrangement in the proximal gonad, failed to enter the spermatheca and become fertilized, and instead underwent several rounds of DNA synthesis, typical of endomitotic oocytes (Emo) (Iwasaki et al., 1996) (Figure 6). In contrast, β*pat-3*(W784A) andβ*pat-3* (FKVV) had very low penetrance of the Emo phenotype, not significantly different from β*pat-3* (+). These results suggest that specific residues in the βPAT-3 cytoplasmic tail are required for optimal contraction of the myoepithelial sheath during ovulation.

Disruption of conserved residues in βPAT-3 cytoplasmic tail leads to defects in tail morphogenesis

Tail morphogenesis was previously assumed to be an integrin-independent process, but to our surprise, the β*pat-3*(TTAA) animals also exhibited abnormal tail morphology. In some transgenic animals, the tails were curved and shortened with a lumpy appearance. These tail shafts were irregularly shaped and often out of focus when observed by microscopy, suggesting that the tails are twisted and curved from the regular position (Figure 7). This phenotype is known as abnormal tail appearance (Abt). Distortion of the musculature can cause a shortened body appearance with abnormal tail structures, including a twisted tail shaft with abnormal, lumpy protrusions (Kramer and Johnson, 1993). The Abt phenotype was also observed less frequently in several of the other lines. In these animals the penetrance of the tail defect was not significantly different from β*pat-3*(+). This is a novel phenotype that has not previously been associated with disruption of integrin function, and may suggest that proper attachment of the tail musculature to the ECM or the underlying hypodermis requires integrin.

Discussion

This study demonstrates that many of the conserved motifs in the cytoplasmic tail ofβ*pat-3* are needed for integrin-regulated functions such as cell migration, cytoskeletal organization, and tissue organization. Surprisingly, disruption of two well conserved motifs, ^{795}FK^{796} and W^{784}, did not result in significant defects, suggesting these conserved residues may not be crucial for function of PAT-3. Disruption of conserved amino acid residues by a frameshift mutation in β*pat-3*(β1C) resulted in a temperature sensitive arrest at larval stages. Although not completely normal, β*pat-3*(β1C) animals grown at the more permissive temperature were much less affected. Point mutations in the NPXY motifs, disruption of the ^{797}TT^{798} motif, or disruption of the C-terminal portion of the cytoplasmic domain in β*pat-3*(β1C) resulted in DTC migration and ovulation defects. Although the mutants showed defects in many tissues, βPAT-3 protein appeared to express and localize properly in dense body structures in body wall muscle, except for the β*pat-3*(β1C) animals that had disrupted actin organization in some muscle cells. An important new finding of this study is the importance of the ^{797}TT^{798} motif for integrin function. In contrast to the other lines, β*pat-3*(TTAA) lines exhibited defects not only in DTC migration and ovulation, but also in tail morphogenesis. This result reveals new integrin functions in tissue morphogenesis, and suggests that specific tissues have enhanced sensitivity to the absence of specific residues, for example ^{797}TT^{798}, in the βPAT-3 cytoplasmic tail.

We do not think the defects observed in this study are attributable to overexpression. Expression of the constructs, with the exception of β*pat-3*(β1C), in the wild type background did not produce defective phenotypes (data not shown). In addition, each construct, although similarly overexpressed, yields an overlapping but distinct set of phenotypes. Conversely, it is possible the phenotypes in these rescued lines are comparatively mild due to compensation by overexpression of the rescue constructs.

Integrin is a versatile cell surface receptor for ECM molecules. In mammalian systems,β1 integrin produces multiple splice variants depending on cellular needs. To date, there are 4 different splice variants which confer distinct functions to the cytoplasmic tails. In *C. elegans*, *βpat-3* splice variant forms have not previously been identified (Gettner et al., 1995), however, *βpat-3* does possess a conserved intron at a similar position in the cytoplasmic tail of mammalian β1 integrin (Gettner et al., 1995; Jannuzi et al., 2002). We created a mutation designed to produce an integrin similar to the β1C variant of mammalian β1 integrin. In the β*pat-3*(β1C) animals, failure to splice out a small intron results in the production of a β*pat-3* cytoplasmic tail 42 aa long that lacks both NPXY motifs. To our surprise, this *βpat-3* construct was able to rescue the embryonic lethality of *βpat-3(st564)*. At the non-permissive temperature, an increase in unspliced transcripts may result in arrest of β*pat-3*(β1C) animals early in larval development. Although β*pat-3*(β1C) displayed a nearly complete larval arrest at 15°C, arrested animals did not have grossly disrupted muscle structure, suggesting that the muscle elongation defects are unlikely the main cause of arrest. Similarity of this phenotype to the larval lethality of *αina-1* null mutants (Baum and Garriga, 1997), suggests proteins translated from unspliced *βpat-3(β1C)* transcript may interfere with *αina-1* function thereby resulting in the observed phenotype. In addition to any dominant effects of the β*pat-3*(β1C) construct, the two NPXY motifs, abolished in the non-spliced form, may be required for development.

Integrins are activated by binding of cytoplasmic factors that alter the conformation of integrins and increase their affinity for ligand (Calderwood, 2004). Binding of cytoplasmic proteins, such as talin, to the C-terminal NPXY motif is an important component of this process, known as inside-out signaling. The TT residues are also known to be involved in inside-out signaling. For example, a TTAA mutation in GD25 cells resulted in defective inside-out signaling in response to fibronectin fibrils (Wennerberg et al., 1998). The TT motif is known to interact with the conserved F3 subdomain of the FERM domain in kindlins, proteins similar to *C. elegans* UNC-112 (Harburger et al., 2009). Surprisingly, the β*pat-3*(TTAA) animals displayed DTC migration defects and protrusions in the tail, but no discernible defects in muscle cytoskeleton. Integrin structures in the *C. elegans* musculature are likely quite stable, remaining engaged with matrix ligands, and therefore may be less susceptible to any deficiencies in inside-out signaling than migratory cells or tissues undergoing larval developmental morphogenesis.

In conclusion, this study, in conjunction with our earlier work, has established an *in vivo* system to study cell adhesion and integrin function in living animals. The panel of transgenic nematodes will provide a valuable resource for the study of cell migration, contraction and morphogenesis. Further studies will address the tissue specific functions of integrin in cell-ECM interactions in these processes.

Materials and Methods

Animals and culture

Nematodes were cultivated on nematode growth medium (NGM) agar plates with OP50 bacteria according to standard techniques (Brenner, 1974). The RW3600 qC1 *dpy-19(e1259)*

glp-1(q339)/pat-3(st564) III (Williams and Waterston, 1994) *C. elegans* strain used in this study were obtained from the Caenorhabditis Genetics Center, St. Paul, MN.

Mutant constructs and germline transformation

pPAT3(+)-PB12K was excised from the ZK1058 cosmid using NEB restriction enzymes PstI and BsrB1 and inserted between PstI and SmaI sites of pSP73 plasmid vector (Promega) (Lee et al., 2001). Corresponding mutant constructs, pPAT3-Y792F, pPAT3-W784A, pPAT3-FKVV, pPAT3-TTAA, and pPAT3-β1C, were created using overlap extension PCR. After the overlap extension PCR, the 754-bp MscI-EcoRI fragments from the PCR were cloned back into the corresponding position of pPAT3-PB12K. Plasmids were isolated and purified by $CsCl_2$ density gradient centrifugation.

Germline transformation was performed as described in Mello *et al.* (Mello et al., 1991). pPAT3 constructs were mixed with TG96 *sur-5::GFP* (Gu et al., 1998) as a coinjection marker. Injections were first attempted at a mixture of 10 μg/ml of pPAT3 and 100 μg/ml of TG96 in TE buffer (pH=7.5). Various injection concentrations were used and lines generated from the lowest possible concentration of the pPAT3 construct were analyzed further. The β*pat-3*(β1C) lines were generated at pPAT3-β1C 50 μg/ml and TG96 50 μg/ml, which was the only concentration found to generate a viable rescue. To rescue β*pat-3(st564)* with the pPAT3 constructs, the distal gonad of RW3600 qC1 *dpy-19(e1259) glp-1(q339)/ pat-3(st564)* III animals was microinjected with the injection mixture. After the initial generation of F1 green worms, those animals were propagated by selfing, a single hermaphrodite growing on a NGM plate. Plates with F2 green progeny were then examined for the further screening; green F2 animals were selfed on individual plates. F2 plates with 100% green progeny were selected for phenotype characterization. Multiple rescued lines were generated, and the lines were allowed to grow for more than 10 generations before characterizing the phenotypes (Lee et al., 2001).

Phenotype characterization

To score fertility, a L4 or young adult transgenic animal was selfed on an OP50 seeded NGM plate. Presence of progeny was scored for 4 consecutive days. To analyze gonad and tail morphology, young adult transgenic hermaphrodites were mounted in a drop of M9 buffer containing 20 mMNaN_3 (Sigma Chemical Co.) on a 24×60 mm coverslip containing wet surface of 3%agarose in water and examined using a Nikon TE2000-U Diaphot microscope with DIC optics. Images were captured using a CoolSnap *cf* monochrome camera (Roper Scientific, Tucson, AZ) and analyzed with Metavue imaging software (version 7.1, Molecular Devices Co, Downingtown, PA). Gonad morphology was scored essentially as previously described (Lee et al., 2001). Young adult hermaphrodites with tail shafts much shorter than normal or tails with protrusions or lumps in the surface cuticular material (Kramer and Johnson, 1993) were scored as possessing the abnormal tail (Abt) phenotype. When oocytes were present in a non-linear arrangement in the proximalgonad of young adult animals, animals were scored as exhibiting the endomitotic oocyte (Emo) phenotype.

Fluorescence microscopy

To visualize βPAT-3 distribution in body wall muscles, transgenic worms were collected in M9 buffer containing 1% sodium azide (NaN_3, w/v). Using a razor blade, worms were diced randomly on a poly-L-lysine (1 mg/ml, w/v) coated slides and fixed with methanol and acetone at −20°C, followed by treatment with MH25, anti-βPAT-3 monoclonal antibody (1:1,00 dilution in M9 buffer with 1% goat serum), overnight at RT. The samples were then treated with a secondary goat anti-mouse IgG FITC conjugated antibody, (Sigma-Aldrich Chem, St. Louis, MO) (1:5,000 dilution in M9 buffer with 1% goat serum), for 2–3 hrs at

RT. The samples were washed and mounted on a Nikon TE2000-U inverted microscope for fluorescence microscopy. For phalloidin staining, animals were dissected on poly-L-lysine coated slide and fixed with methanol and acetone. Fixed worms were the treated with rhodamine-conjugated phalloidin (1:200 dilution, Fluka Science) in M9 buffer for 2 to 3 hours at RT. Prepared samples were observed on the Nikon TE2000-U diaphot microscope. Images were captured using a CoolSnap *cf* monochrome camera (Roper Scientific, Tucson, AZ) and analyzed with Metavue imaging software (version 5, Molecular Devices Co, Downingtown, PA).

Reverse transcription PCR (RT-PCR)

To analyze β*pat-3* transcripts, transgenic worm lines, N2, JE443 β*pat-3*(+) and BU7221β*pat-3*(β1C) were then collected with M9 buffer and frozen in liquid nitrogen. Frozen worm pellets were ground to a powder with a mortar and pestle. Worms were extracted with Tri-Reagent (Sigma-Aldrich, St. Louis, MO) and chloroform (1.5 volumes) and RNA was precipitated from the extract with ethanol and 3 M sodium acetate. After an ethanol rinse, the RNA was treated with RQ1 DNase (Promega, Madison, WI) to remove contaminating DNA. Approximately 1 μg of total RNA was used to synthesize cDNA with the Transcriptor Reverse Transcription Kit (Roche, Carlsbad, CA) primed with random hexamers in a 20 μl reaction. 1–2 μl cDNA was subsequently used in PCR amplification with β*pat-3* primers and also with control GAPDH primers to amplify the. *C. elegans* gene T09F3.3 (GAPDH). Primer sequences listed below were used for amplification:

PAT3PT Forward 1: 5′-ctcaacgaaactacaccctgcc-3′

PAT3PT Reverse 1: 5′-ttagttggcttttccagcgtatactgg-3′

PAT6 Forward: 5′-gctagctcctggtgcttcttg-3′

PAT6 Reverse: 5′-aagcttctcctcgtggctttg-3′

PCR products were then inserted into pGEM-T vector and transformed into DH5α bacteria (Invitrogen, Carlsbad, CA). Isolated plasmids containing the PCR products were sent to Macrogen (Bethesda, MD) for sequencing service and sequence data were analyzed by BLASTn search. For qPCR analysis, 1 μl cDNA was used in each reaction with iQ SYBRgreen Supermix (Bio-Rad Laboratories, Hercules, CA) in a 96-well plate. Amplification of *C. elegans* gene *ama-1* was used as a loading and amplification control. All assays were amplified and evaluated in real time using an ABI Prism 7000 sequence detection system. The relative quantitation of *pat-3* mRNA was calculated by the comparative Ct method (Livak and Schmittgen, 2001).

Acknowledgments

C. elegans strains were provided by the Caenorhabditis Genetics Center, which is funded by the NIH. Authors thank Julia Lee for technical assistance. This work was supported by funds from Baylor University and a research grant from NIH (GM077156) for M. Lee.

Grant Sponsor: NIH NIGMS # GM077156 for M. Lee.

References

Argraves WS, Suzuki S, Arai H, Thompson K, Pierschbacher MD, Ruoslahti E. Amino acid sequence of the human fibronectin receptor. J Cell Biol. 1987; 105:1183–1190. [PubMed: 2958481]

Aroian RV, Koga M, Mendel JE, Ohshima Y, Sternberg PW. The let-23 gene necessary for Caenorhabditis elegans vulval induction encodes a tyrosine kinase of the EGF receptor subfamily. Nature. 1990; 348:693–699. [PubMed: 1979659]

Aroian RV, Levy AD, Koga M, Ohshima Y, Kramer JM, Sternberg PW. Splicing in Caenorhabditis elegans does not require an AG at the 3′ splice acceptor site. Mol Cell Biol. 1993; 13:626–637. [PubMed: 8417357]

Aroian RV, Sternberg PW. Multiple functions of let-23, a Caenorhabditis elegans receptor tyrosine kinase gene required for vulval induction. Genetics. 1991; 128:251–267. [PubMed: 2071015]

Baum PD, Garriga G. Neuronal migrations and axon fasciculation are disrupted in *ina-1* integrin mutants. Neuron. 1997; 19:51–62. [PubMed: 9247263]

Belkin AM, Retta SF. beta1D integrin inhibits cell cycle progression in normal myoblasts and fibroblasts. J Biol Chem. 1998; 273:15234–15240. [PubMed: 9614138]

Belkin AM, Retta SF, Pletjushkina OY, Balzac F, Silengo L, Fassler R, Koteliansky VE, Burridge K, Tarone G. Muscle β1D integrin reinforces the cytoskeleton-matrix link: Modulation of integrin adhesive function by alternative splicing. J Cell Biol. 1997; 139:1583–1595. [PubMed: 9396762]

Brenner S. The genetics of *Caenorhabditis elegans*. Genetics. 1974; 77:71–94. [PubMed: 4366476]

Calderwood DA. Talin controls integrin activation. Biochem Soc Trans. 2004; 32:434–437. [PubMed: 15157154]

Calderwood DA, Yan B, de Pereda JM, Alvarez BG, Fujioka Y, Liddington RC, Ginsberg MH. The phosphotyrosine binding-like domain of talin activates integrins. J Biol Chem. 2002; 277:21749–21758. [PubMed: 11932255]

Chen H, Zou Z, Sarratt KL, Zhou D, Zhang M, Sebzda E, Hammer DA, Kahn ML. In vivo beta1 integrin function requires phosphorylation-independent regulation by cytoplasmic tyrosines. Genes Dev. 2006; 20:927–932. [PubMed: 16618804]

Chen WJ, Goldstein JL, Brown MS. NPXY, a sequence often found in cytoplasmic tails, is required for coated pit-mediated internalization of the low density lipoprotein receptor. J Biol Chem. 1990; 265:3116–3123. [PubMed: 1968060]

Cram EJ, Clark SG, Schwarzbauer JE. Talin loss-of-function uncovers roles in cell contractility and migration in *C. elegans*. J Cell Sci. 2003; 116:3871–3878. [PubMed: 12915588]

Cram EJ, Shang H, Schwarzbauer JE. A systematic RNA interference screen reveals a cell migration gene network in C. elegans. J Cell Sci. 2006; 119:4811–4818. [PubMed: 17090602]

Czuchra A, Meyer H, Legate KR, Brakebusch C, Fassler R. Genetic analysis of beta1 integrin “activation motifs” in mice. J Cell Biol. 2006; 174:889–899. [PubMed: 16954348]

Fornaro M, Manzotti M, Tallini G, Slear AE, Bosari S, Ruoslahti E, Languino LR. Beta1C integrin in epithelial cells correlates with a nonproliferative phenotype: forced expression of beta1C inhibits prostate epithelial cell proliferation. Am J Pathol. 1998; 153:1079–1087. [PubMed: 9777939]

Fornaro M, Steger CA, Bennett AM, Wu JJ, Languino LR. Differential role of beta(1C) and beta(1A) integrin cytoplasmic variants in modulating focal adhesion kinase, protein kinase B/AKT, and Ras/Mitogen-activated protein kinase pathways. Mol Biol Cell. 2000; 11:2235–2249. [PubMed: 10888665]

Fornaro M, Zheng DQ, Languino LR. The novel structural motif Gln795-Gln802 in the integrin beta 1C cytoplasmic domain regulates cell proliferation. J Biol Chem. 1995; 270:24666–24669. [PubMed: 7559578]

Francis R, Waterston RH. Muscle cell attachment in *Caenorhabditis elegans*. J Cell Biol. 1991; 114:465–479. [PubMed: 1860880]

Gettner, SN. Isolation and functional analysis of Caenorhabditis elegans integrin βpat-3. San Francisco, CA: University of California; 1994.

Gettner SN, Kenyon C, Reichardt LF. Characterization of βpat-3 heterodimers, a family of essential integrin receptors in *C. elegans*. J Cell Biol. 1995; 129:1127–1141. [PubMed: 7744961]

Giancotti FG. Integrin signaling: specificity and control of cell survival and cell cycle progression. Curr Opin Cell Biol. 1997; 9:691–700. [PubMed: 9330873]

Giancotti FG, Ruoslahti E. Integrin signaling. Science. 1999; 285:1028–1032. [PubMed: 10446041]

Gu T, Orita S, Han M. *Caenorhabditis elegans* SUR-5, a novel but conserved protein, negatively regulates LET-60 Ras activity during vulval induction. Molecular and Cellular Biolgy. 1998; 18:4556–4564.

Harburger DS, Bouaouina M, Calderwood DA. Kindlin-1 and -2 directly bind the C-terminal region of beta integrin cytoplasmic tails and exert integrin-specific activation effects. J Biol Chem. 2009; 284:11485–11497. [PubMed: 19240021]

Hirsch E, Barberis L, Brancaccio M, Azzolino O, Xu D, Kyriakis JM, Silengo L, Giancotti FG, Fassler R, Altruda F. Defective Rac-mediated proliferation and survival targeted mutation of the β1 integrin cytodomain. J Cell Biol. 2002; 157:481–492. [PubMed: 11980921]

Hubbard EJ, Greenstein D. The *Caenorhabditis elegans* gonad: a test tube for cell and developmental biology. Dev Dyn. 2000; 218:2–22. [PubMed: 10822256]

Hynes RO. Integrins: Versatility, modulation and signaling in cell adhesion. Cell. 1992; 69:11–25. [PubMed: 1555235]

Hynes RO. Integrins: bidirectional, allosteric signaling machines. Cell. 2002; 110:673–687. [PubMed: 12297042]

Iwasaki K, McCarter J, Francis R, Schedl T. *emo-1*, a *Caenorhabditis elegans* Sec61p gamma homologue, is required for oocyte development and ovulation. J Cell Biol. 1996; 134:699–714. [PubMed: 8707849]

Jannuzi AL, Bunch TA, Brabant MC, Miller SW, Mukai L, Zavortink M, Brower DL. Disruption of C-terminal cytoplasmic domain of betaPS integrin subunit has dominant negative properties in developing Drosophila. Mol Biol Cell. 2002; 13:1352–1365. [PubMed: 11950944]

Jannuzi AL, Bunch TA, West RF, Brower DL. Identification of integrin beta subunit mutations that alter heterodimer function in situ. Mol Biol Cell. 2004; 15:3829–3840. [PubMed: 15194810]

Kaapa A, Peter K, Ylanne J. Effects of mutations in the cytoplasmic domain of integrin beta(1) to talin binding and cell spreading. Exp Cell Res. 1999; 250:524–534. [PubMed: 10413605]

Kramer, JM. Extracellular Matrix. In: Riddle, DL.; Blumenthal, T.; Meyer, BJ.; Priess, JR., editors. C elegans II. Cold Spring Harbor: Cold Spring Harbor Laboratory Press; 1997. p. 471-500.

Kramer, JM. Basement membranes. WormBook; 2005. p. 1-15.

Kramer JM, Johnson JJ. Analysis of mutations in the sqt-1 and rol-6 collagen genes of Caenorhabditis elegans. Genetics. 1993; 135:1035–1045. [PubMed: 8307321]

Law DA, DeGuzman FR, Heiser P, Ministri-Madrid K, Killeen H, Phillips DR. Integrin cytoplasmic tyrosine motif is required for outside-in αIIbβ3 signalling and platelet function. Nature. 1999; 401:808–811. [PubMed: 10548108]

Lee M, Cram EJ, Shen B, Schwarzbauer JE. Role of βpat-3 integrins in development and function of *Caenorhabditis elegans* muscles and gonads. J Biol Chem. 2001; 276:36404–36410. [PubMed: 11473126]

Lee M, Shen B, Schwarzbauer JE, Ahn J, Kwon J. Connections between integrins and Rac GTPase pathways control gonad formation and function in *C. elegans*. Biochim Biophys Acta. 2005; 1723:248–255. [PubMed: 15716039]

Livak KJ, Schmittgen TD. Analysis of relative gene expression data using real-time quantitative PCR and the 2(−Delta Delta C(T)) Method. Methods. 2001; 25:402–408. [PubMed: 11846609]

Manzotti M, Dell'Orto P, Maisonneuve P, Fornaro M, Languino LR, Viale G. Down-regulation of beta(1C) integrin in breast carcinomas correlates with high proliferative fraction, high histological grade, and larger size. Am J Pathol. 2000; 156:169–174. [PubMed: 10623664]

Meighan CM, Schwarzbauer JE. Control of C. elegans hermaphrodite gonad size and shape by vab-3/Pax6-mediated regulation of integrin receptors. Genes Dev. 2007; 21:1615–1620. [PubMed: 17606640]

Mello CC, Kramer JM, Stinchcomb D, Ambros V. Efficient gene transfer in *C. elegans*: extrachromosomal maintenance and integration of transforming sequences. EMBO J. 1991; 10:3959–3970. [PubMed: 1935914]

Meredith J Jr, Takada Y, Fornaro M, Languino LR, Schwartz MA. Inhibition of cell cycle progression by the alternatively spliced integrin beta 1C. Science. 1995; 269:1570–1572. [PubMed: 7545312]

Moerman, DG.; Williams, BD. Sarcomere assembly in C elegans muscle. WormBook; 2006. p. 1-16.

Montell DJ. The genetics of cell migration in *Drosophila melanogaster* and *Caenorhabditis elegans* development. Development. 1999; 126:3035–3046. [PubMed: 10375496]

Nishiwaki K. Mutations affecting symmetrical migration of distal tip cells in *Caenorhabditis elegans*. Genetics. 1999; 152:985–997. [PubMed: 10388818]

Oxley CL, Anthis NJ, Lowe ED, Vakonakis I, Campbell ID, Wegener KL. An integrin phosphorylation switch: the effect of beta3 integrin tail phosphorylation on Dok1 and talin binding. J Biol Chem. 2008; 283:5420–5426. [PubMed: 18156175]

Pankov R, Cukierman E, Clark K, Matsumoto K, Hahn C, Poulin B, Yamada KM. Specific beta1 integrin site selectively regulates Akt/protein kinase B signaling via local activation of protein phosphatase 2A. J Biol Chem. 2003; 278:18671–18681. [PubMed: 12637511]

Sakai T, Zhang Q, Fassler R, Mosher DF. Modulation of β1A integrin functions by tyrosine residues in the β1 cytoplasmic domain. J Cell Biol. 1998; 141:527–538. [PubMed: 9548729]

Sherwood DR, Butler JA, Kramer JM, Sternberg PW. FOS-1 promotes basement-membrane removal during anchor-cell invasion in C. elegans. Cell. 2005; 121:951–962. [PubMed: 15960981]

Tanentzapf G, Brown NH. An interaction between integrin and the talin FERM domain mediates integrin activation but not linkage to the cytoskeleton. Nat Cell Biol. 2006; 8:601–606. [PubMed: 16648844]

Wennerberg A, Fassler R, Warmegard B, Johansson S. Mutational analysis of the potential phosphorylation sites in the cytoplasmic domain of integrin β1A. Journal of Cell Science. 1998; 111:1117–1126. [PubMed: 9512507]

Williams BD, Waterston RH. Genes critical for muscle development and function in *Caenorhabditis elegans* identified through lethal mutations. J Cell Biol. 1994; 124:475–490. [PubMed: 8106547]

Xu X, Lee D, Shih HY, Seo S, Ahn J, Lee M. Linking integrin to IP(3) signaling is important for ovulation in *Caenorhabditis elegans*. FEBS Lett. 2005; 579:549–553. [PubMed: 15642374]

Xu X, Rongali SC, Miles JP, Lee KD, Lee M. *pat-4*/ILK and *unc-112*/Mig-2 are required for gonad function in *Caenorhabditis elegans*. Exp Cell Res. 2006; 312:1475–1483. [PubMed: 16476426]

Zawistowski JS, Serebriiskii IG, Lee MF, Golemis EA, Marchuk DA. KRIT1 association with the integrin-binding protein ICAP-1: a new direction in the elucidation of cerebral cavernous malformations (CCM1) pathogenesis. Hum Mol Genet. 2002; 11:389–396. [PubMed: 11854171]

Zusman S, Grinblat Y, Yee G, Kafatos FC, Hynes RO. Analyses of PS integrin functions during Drosophila development. Development. 1993; 118:737–750. [PubMed: 8076515]

Zusman S, Patel-King RS, Ffrench-Constant C, Hynes RO. Requirements for integrins during Drosophila development. Development. 1990; 108:391–402. [PubMed: 2340808]

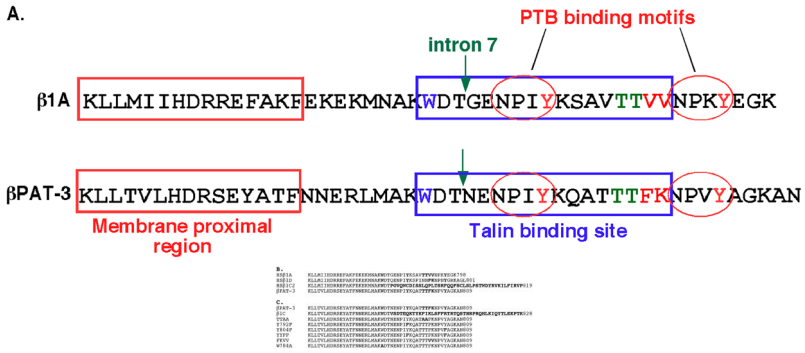

Figure 1. Conserved residues in the *C. elegans*βPAT-3 cytoplasmic tail

(A) Amino acid residues in βPAT-3 cytoplasmic tail sequence and their functions. The amino acid sequence of the entire cytoplasmic domain of human integrin β1A (top) is aligned with βPAT-3 (bottom). The membrane proximal region (red box) and talin binding site (blue box) are indicated. Conserved features targeted in this study are βPAT-3 ^{784}W (blue), the NPXY motifs (red ovals), the ^{797}TT^{798} (green), the ^{799}FK^{800} (red) motif, and a splice junction mutant (green arrow, intron 8) that introduces a frame shift.

(B) Alignment of the amino acid sequences of *C. elegans* βPAT-3 and human β1A, β1D and β1C cytoplasmic tails. Residues relevant to this study are in bold.

(C) Sequences of the βPAT-3 cytoplasmic domain mutants analyzed in this study.

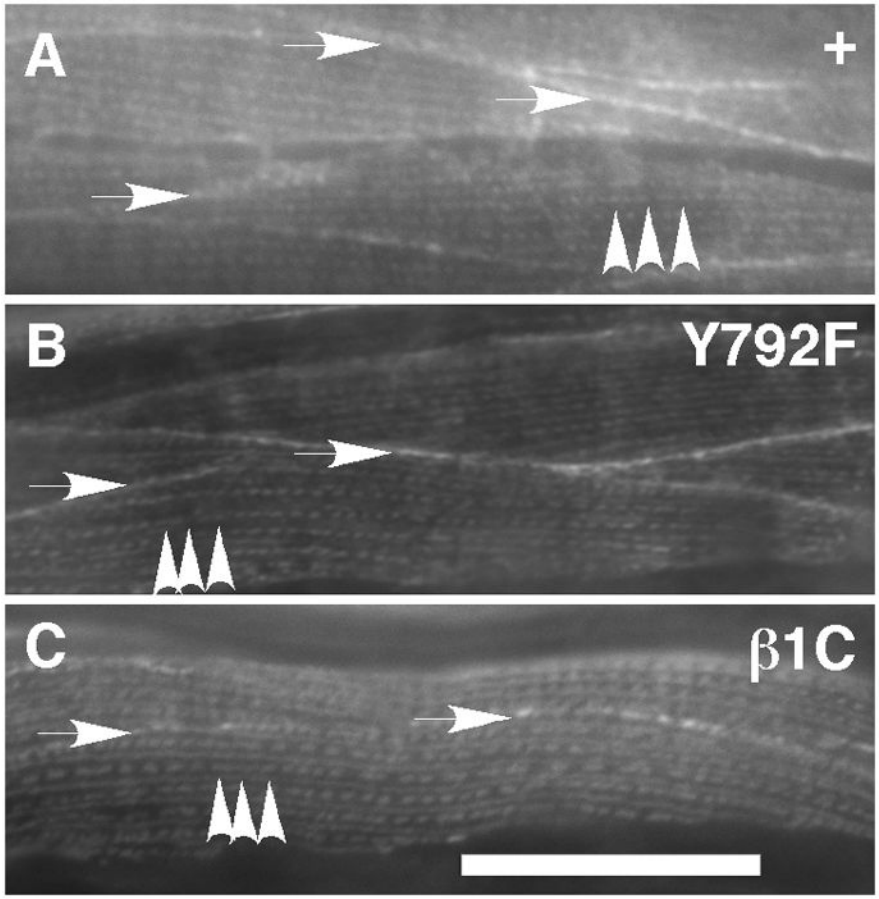

Figure 2. βPAT-3 localizes normally in muscle cells of rescued animals

(A) βPAT-3 in rescued lines was detected by immunofluorescence with MH25 antibodies. Typical dense body (arrowheads) and cell-to-cell contacts (arrows) were observed in the muscle cells. The staining pattern was similar to N2 (data not shown). This typical MH25 staining pattern was observed in other transgenic lines such as (B) β*pat-3*(Y792F) and (C) β*pat-3*(β1C). Scale bars= 40 μm.

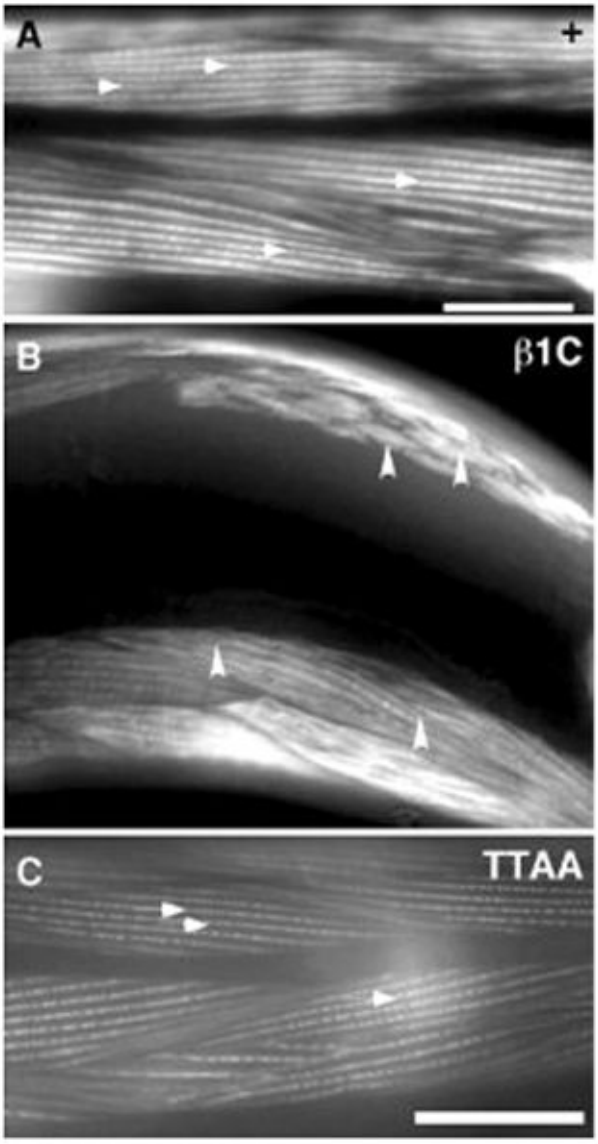

Figure 3. Visualization of actin structure in muscle cells of rescued animals

(A) Staining of β*pat-3*(+) transgenic animals with rhodamine-phalloidin revealed a normal pattern of filamentous actin (arrows). However, (B) rescue with βpat-3(β1C) resulted in clumped actin filaments (arrowheads). Some of the muscle cells also appeared irregularly shaped. In contrast, animals rescued with (C) β*pat-3*(TTAA), had normal actin filaments. Scale bars = 40μm.

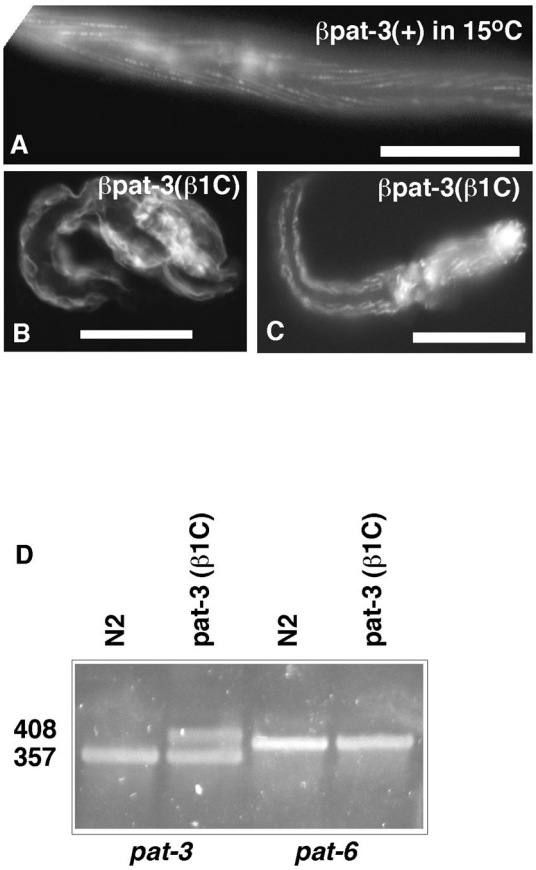

Figure 4. Characterization β*pat-3* (β1C) defects

β*pat-3*(+) and β*pat-3*(β1C) mutant animals were propagated at 15°C. β*pat-3*(+) (A) and β*pat-3* (β1C) (B, C) L2 animals were stained with rhodamine-phalloidin to visualize actin. Arrestedβ*pat-3*(β1C) animals appeared to have disorganized body wall muscle (B, C). RNA from these mutant worms was isolated to confirm the expression of mutant integrin mRNA. In panels (A), (B), and (C), bars indicate 40 μm. (D) In contrast to the expected wild type cDNA size expected (N2 lane), cDNA prepared from β*pat-3*(β1C) animals displayed two bands specific for β*pat-3* (β*pat-3*(β1C) lane). These products were sequenced and confirmed to represent spliced and unspliced β*pat-3* message. *pat-6* was amplified in parallel as a control to show the level of cDNA and residual genomic DNA (almost undetectable) in the samples.

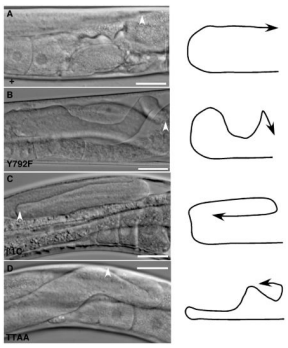

Figure 5. β*pat-3* transgenic animals display DTC migration defects

Normal DTC migration in a (A) β*pat-3* (+) rescued animal in contrast to the (B) β*pat-3*(Y972F), (C) β*pat-3*(β1C), and (D) β*pat-3*(TTAA) rescued lines, in which the DTC (arrowhead) follows an incorrect migratory path. The path taken by the DTC is indicated by the arrow diagrams. In all panels, vulva is located on the bottom right corner. Scale bars = 40 μm.

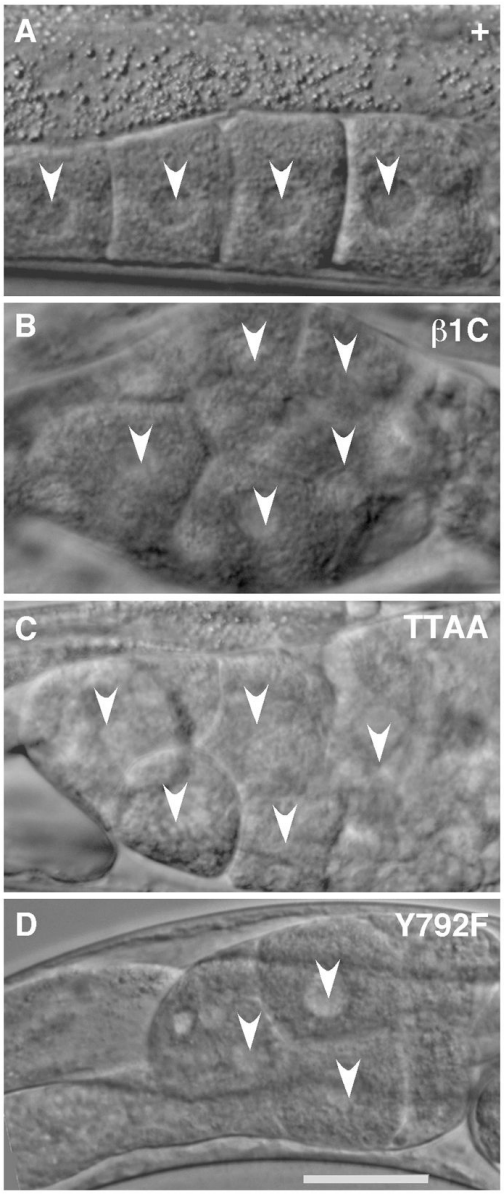

Figure 6. Proximal gonad morphology of β*pat-3* transgenic animals

(A) β*pat*- (+) line possessed normally developing oocytes arranged in a typical linear pattern. In the (B) β*pat-3*(β1C), (C) β*pat-3*(TTAA), and (D) β*pat-3*(Y792F) lines, oocytes failed to ovulate and piled on top of each other in the proximal gonad, a phenotype typical of endomitotic (Emo) oocytes. Arrowheads indicate the oocyte nuclei. Scale bar = 40 μm.

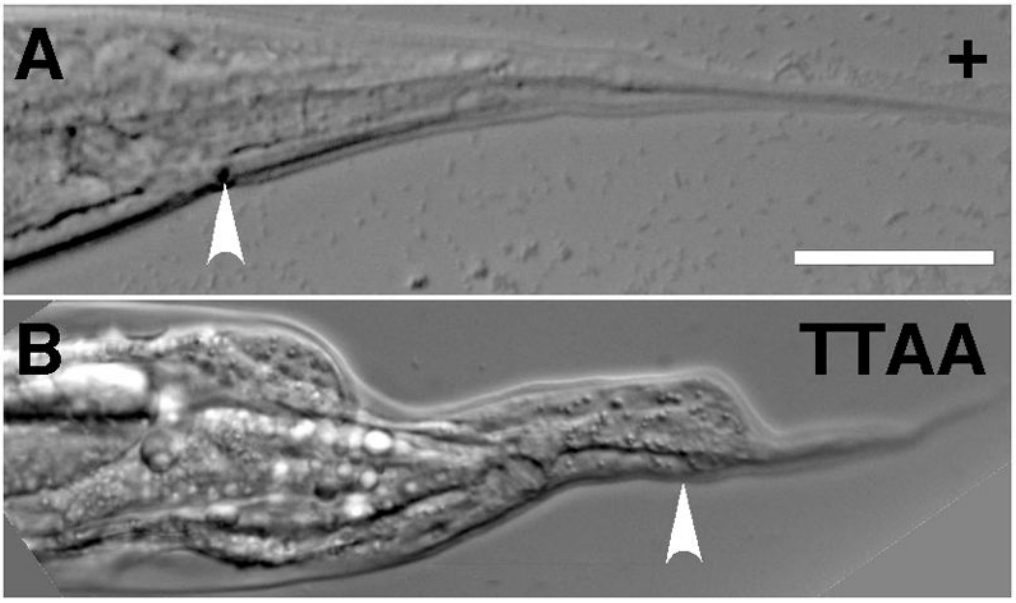

Figure 7. Abnormal tail (Abt) phenotype of β*pat-3* transgenic animals

(A) A typical wild-type, whiplike hermaphrodite tail of β*pat-3*(+) hermaphrodites. (B) βpat-3(TTAA) animals displayed severely abnormal tail morphology. Arrowheads indicate the location of the anus. Scale bar = 40 μm.

Table 1

βPAT-3 cytoplasmic tail residues are required for fertility, gonad morphogenesis and function, and tail morphogenesis

Young adult animals were scored for fertility (% of animals bearing live progeny), DTC migration defects (% of incorrectly formed gonad arms), Emo (% of animals with endomitotic oocytes) and Abt (% of animals with abnormal tail morphology). Strains showing significant pair-wise differences from wild type (+) for each phenotype, based on the 95% confidence interval for proportions, are shown shaded in gray.

Trait	+	β1C 23°	β1C 15°	TTAA	Y792F	Y804F	YYFF	FKVV	W784A
Fertility	86% N=59	54% N=56	1% N=100	72% N=142	84% N=44	93% N=55	86% N=59	83% N=48	100% N=60
DTC migration	11% N=122	24% N=58	50% N=26	45% N=101	22% N=134	38% N=202	27% N=148	19% N=88	21% N=100
Emo	1% N=112	18% N=129	N.D.	14% N=59	12% N=126	19% N=104	19% N=100	2% N=100	3% N=146
Abt	14% N=59	23% N=56	N.D.	68% N=133	18% N=44	5% N=55	22% N=59	4% N=48	4% N=98